Experimental Determination of the Thermal Conductivity of New Compressed Clay Formulations Stabilized with Gum Arabic, Measurement and Impact on Summer Comfort

Jean Louis Tanguier[1], Abakar Ali[1,2,3], Abdallah Dadi Mahamat[4], André Donnot[1*] and Jean Michel Drouet[2]

[1]*Université de Lorraine, Laboratoire d'Etudes et de Recherches sur le Matériaux Bois (LERMAB), 54500 Vandœuvre-Lès-Nancy, France.*
[2]*Département de langues, Université de Lorraine, 54500 Vandoeuvre les Nancy, France.*
[3]*Ecole Nationale Supérieure des Travaux Publics (ENSTP), BP 60, Njamena, Chad.*
[4]*Departement de Genie Energetique, Institut National Superieur des Sciences et Techniques d'Abeche (INSTA), BP 130, Abeche, Chad.*

Authors' contributions

This work was carried out in collaboration among all authors. Author JLT performed the statistical analysis, wrote the protocol, and wrote the first draft of the manuscript. Author AA performed the studies, primary results analysis and bibliography. Authors ADM and AD managed the analyses of the study. Author JMD managed external reviews and translation adequacy. All authors read and approved the final manuscript.

Article Information

Original Research Article

ABSTRACT

Our work expressed that compressed and stabilized clay with arabic gum is a suitable building material in regards to the mechanical properties. This paper presents an experimental study of the determination of thermal conductivity in a steady state cylindrical geometry configuration approach.

The results obtained give a thermal conductivity in the order of 1 W.m^{-1}. K^{-1}, quite similar to other building materials. On the other hand, because of its inertia, the material dampens the temperature variations between the inside and the outside.

_____

Corresponding author: Email: andre.donnot@univ-lorraine.fr;

NOMENCLATURES

i	inner index	-
e	outer index	-
E	Thermal effusivity	$J.K^{-1}.m^{-2}.s^{-1/2}$
hcv	Convective exchange coefficient	$W.m^{-2}.K^{-1}$
$hray$	Radiative exchange coefficient	$W.m^{-2}.K^{-1}$
Nu	Nusselt number	-
P	Electrical power	W
r	Radius of the block	m
R	Electrical resistance	Ω
T	Temperature	$°C$
W	Moisture content	$\%$
α	Thermal diffusivity	$m^{2}.s^{-1}$
ε	Emissivity	-
λ	Thermal conductivity	$W.m^{-1}.K^{-1}$
σ	Boltzmann constant	$W.m^{-2}.K^{4}$
Φ	Heat flow	W
10/12	Copper tube (10 mm inner diameter / 12 mm outer diameter).	

1. INTRODUCTION

The earth climate evolution is mainly attributed to human energy consumption of fossils fuel. The part of building into the total emitted greenhouse gases is nearly 6% in sub saharian Africa [1] (World Bank Open Data). This part of energy could be easily decreased by substituting cement with local building matter.

Our work aims to enhance local materials which are sustainable, widely available and without negative effects on the environment. We are particularly interested in compressed clay blocks (CCB) stabilized with gum arabic. The first part of our work [2,3] concerns the study of their mechanical properties. Bending-compression measurements are made on cylindrical samples. The material stabilized with 10-15% of gum arabic has a compressive strength that can reach 2.5 MPa and presents good durability when exposed to water.

In the present study, we proceed to the measurement of the thermal properties of our clay-based formulations by measuring their thermal conductivity. Our goal is to check if this material will ensure a good level of comfort in buildings. These values will be used in dynamic thermal simulation (DTS) software (Pleiades developed by IZUBA Energies) to predict the thermal behavior of such a building.

On this subject the literature presents various steady-state methods to measure the conductivity of insulating and granular media [4]. They consist in supposing the medium in thermal equilibrium, and subjected to a stationary flow as a function of time. The measurement is based on processing temperature measurements at different points in the middle. Other methods could also be mentioned, such as the guarded hot plate method [5-7], the bar method [8], the box method [9-12] and the radial flux method [13-15]. All these methods present experimental difficulties such as:

- the existence of contact resistance,
- radial and axial leaks,
- the difficulties of measuring the temperature
- the homogeneity of the temperature field, etc.

The number of samples is important. Also the method must be simple to implement while being sufficiently precise. We have chosen to carry out our measurements in a cylindrical geometry with imposed heat flow in the radial direction. We rely

on the standard NF EN 12390 [16] which recommends cylindrical samples of 160 mm in diameter and 320 mm in length (same dimensions as for the study of physical properties).

This geometry has a better section to lateral surface ratio (0.04 m² / 0.16 m²) and thus allows limiting axial losses. We will check that the contact resistances (thermocouples/material) are weak.

2. MATERIALS AND METHODS

2.1 Thermal Conductivity of a Cylindrical Wall

Steady, in a cylindrical coordinate system, the heat equation is written:

$$\Delta T \equiv \nabla^2 T = 0 \tag{1}$$

Thus : $$\frac{1}{r}\frac{\partial}{\partial r}\left(r\frac{\partial T}{\partial r}\right) + \frac{1}{r^2}\frac{\partial^2 T}{\partial \theta^2} + \frac{\partial^2 T}{\partial z^2} = \tag{2}$$

Considering the cylinder infinite (H > 2D),which is justified by the application of insulation on the 2 sections, the problem becomes one dimensional

$$T(r, \theta, x) = T(r), \tag{3}$$

The equation then becomes: $\frac{1}{r}\frac{\partial}{\partial r}\left(r\frac{\partial T}{\partial r}\right) = 0$

For a cylindrical geometry, in stationary regime and without production of heat, the distribution of the radial temperature is deduced from the equation :

$$T(r) = A\ln(r) + B \tag{4}$$

A and B are determined by the boundary conditions of the problem :

$$T(r = r_i) = T_i \quad T(r = r_e) = T_e \tag{5}$$

Thus : $$A = \frac{T_i - T_0}{\ln\left(\frac{r_i}{r_0}\right)} \quad B = T_i + \frac{T_i - T_0}{\ln\left(\frac{r_i}{r_0}\right)}\ln r_i \tag{6}$$

The integration of the equation between the radiuses r_1 and r_2 amounts to writing the conservation of heat as follows :

$$\int_{r_1}^{r_2}\frac{dr}{r} = \int_{T_1}^{T_2}\frac{-2\pi L\lambda}{\Phi}\,dT \tag{7}$$

Assuming λ independent of temperature in our limit, the thermal conductivity value is expressed as a function of heat flow, temperatures and geometrical magnitudes :

$$\lambda = \frac{\Phi\ln\left(\frac{r_{ext}}{r_{int}}\right)}{2\pi L(T_{int} - T_{ext})} \tag{8}$$
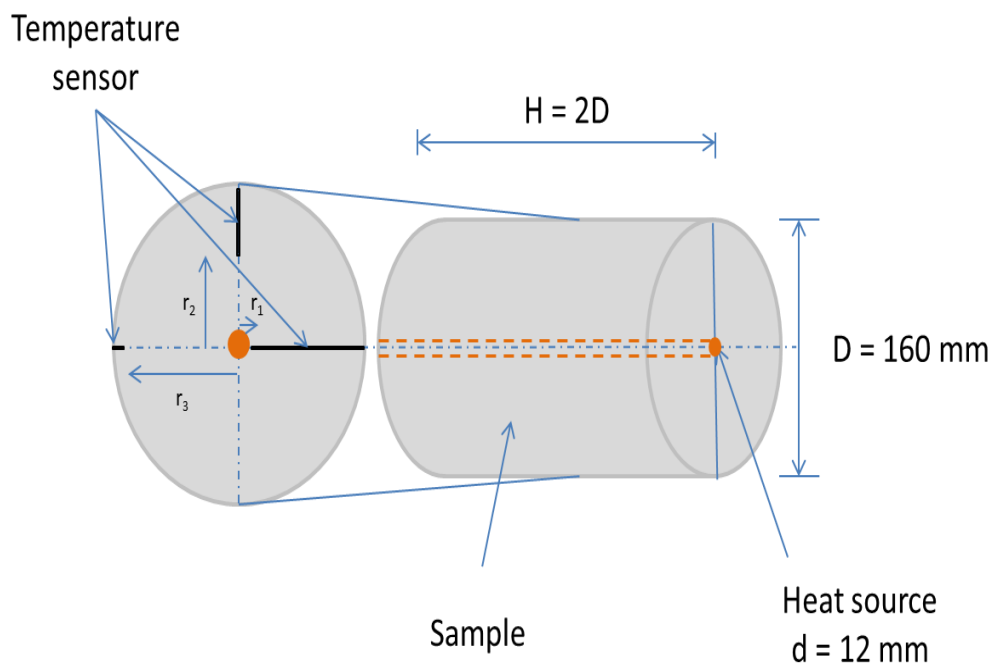

Fig. 1. Position of the thermocouples in the PVC test tube

2.2 Working Hypotheses

For a given body the thermal conductivity value can be influenced by the temperature and the presence of impurities. We consider that our samples are homogeneous and isotropic. This result is obtained by a thorough mixing of the materials used for the different formulations before making the test pieces.

We analyze the results when steady state is established. This brings our technique closer to the hot plate technique.

The cylindrical geometry allows a radial diffusion of heat. The longitudinal component is limited by a surface ratio of 25 %. In addition, the ends of the cylinder are placed between 150 mm thick graphite polystyrene blocks, with a thermal resistance of 4.7 m².K.W^{-1}, which leads to a reduction of 95% of the flow (i.e. an end Rth / lateral Rth =30).

The heat source in the axial position is a special ACIM JOUANIM stainless steel heating cartridge which is 10 mm in diameter, 320 mm length and has a power of 50 W at 230 V. A 10/12 copper tube serves as an interface between the cartridge and the clay. Its role is to even out the temperature on the inside of the test piece and to limit the copper-clay contact resistance. The tube is inserted in the mold before the clay which will be compacted. Good thermal contact between the heating cartridge and the copper is ensured by a thermal grease "Patherm 712" (10 W.m^{-1}.K^{-1}).

The temperature measurements are performed with jacketed,1 mm diameter, type K thermocouples with insulated hot welding.

Clay has a thermal conductivity in the order of 0.7 W.m^{-1}.K^{-1} which can vary with its moisture [17]. Specimens are dried in the open air for a week and then stewed 3 days at 60°C. The samples are weighed to follow the evolution of their mass. After 3 days, it remains constant and we do not notice withdrawal.

2.3 Experimental Device

The diagram of the experimental device is given in Fig. 2. It consists of:

- ➢ A special 10 mm diameter stainless steel 50 W ACIM JOUANIM heating cartridge (320 mm length).
- ➢ A 10/12 copper tube.

- ➢ Jacketed, 1 mm diameter, Type K Thermocouples with insulated hot welding and a accuracy within ± 0.1°C. The acquisition of data (temperatures) is obtained through a previously calibrated ALMEMO 2290-8 acquisition unit.
- ➢ Voltage and current are measured by a BBC M 2042 precision multimeter (± 0.2%).
- ➢ The voltage is adjusted by a variable transformer.

Thermocouples are introduced radially into drilled wells. The position of the thermocouples is as shown in Fig 1. It is meticulously checked for each specimen.

The insulation of the ends of the sample is made with a block of 150 mm thick polystyrene graphite

$$(\lambda = 0.032 \text{ W.m}^{-1}.\text{K}^{-1}).$$

2.4 Verification of Heating Cartridge Capacities in Air

We performed a calibration of the heating cartridge embedded in the copper tube to have an idea of the temperature of the latter in relation to the supply voltage. The results are given in Fig. 3.

The regression law proposed for power versus voltage is: P(W) = 0.0011 × U$^{1.9895}$which corresponds to taking into account the evolution of electrical resistance with temperature.

The NiC80 resistive element (80% Ni, 20% Cr) has a temperature coefficient $\square$ = 0.00017 K^{-1}. Its resistance evolves with temperature according to the law: R = R$_0$ × [1 + α × (T-T$_0$)], with a resistance R$_0$ = 950Ω.

When the heat source is introduced in the PVC block, this causes, at equal tension, an increase in the surface temperature of the copper, It is caused by the thermal resistance of the material.

From the temperature readings on the surface of the copper in air, we calculated the flux exchanged by its surface to check whether it is in concordance with the electric power consumed (cf Table 1)
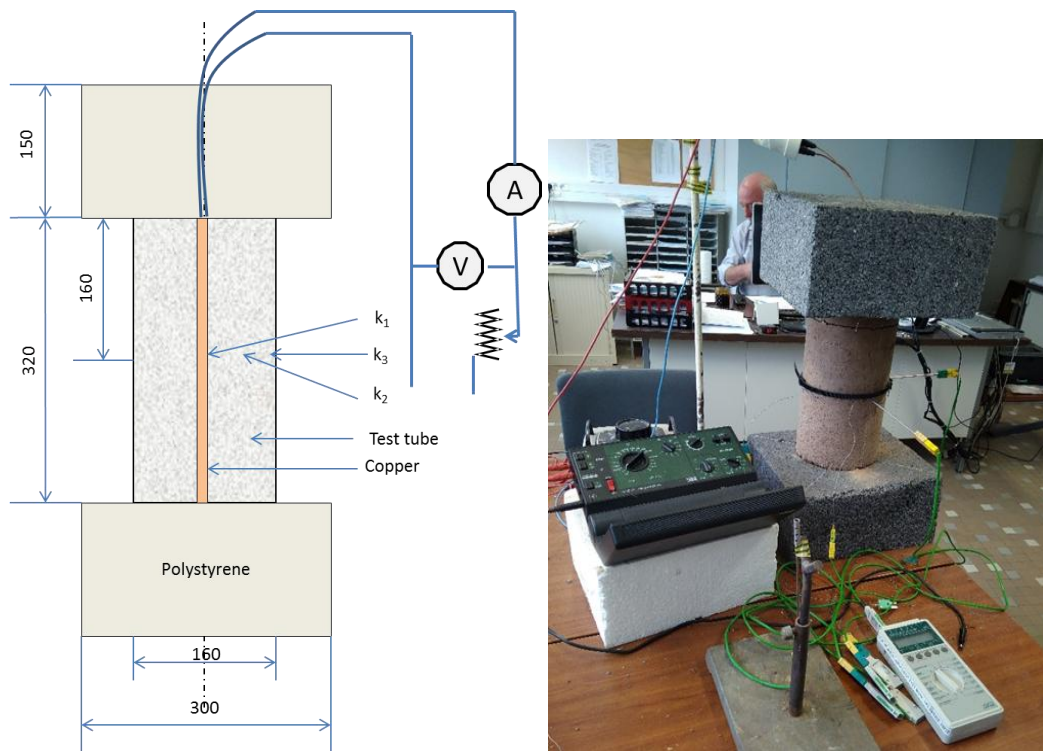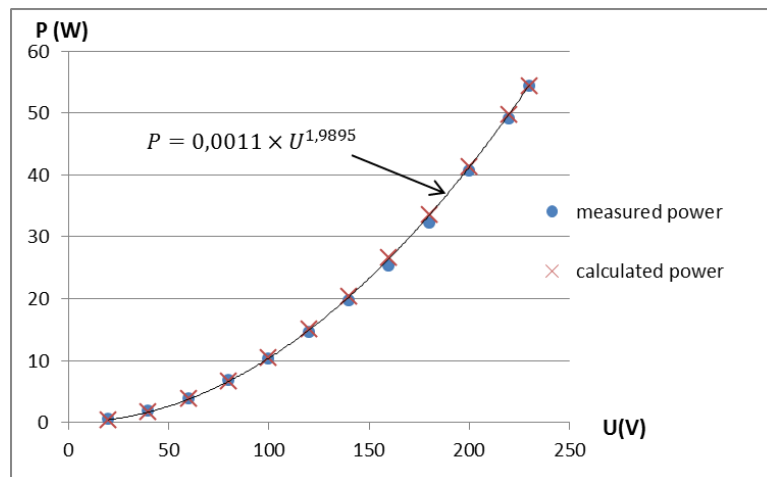
Fig. 2. Experimental Device

Fig. 3. Power versus voltage

We consider a horizontal cylinder exchanging with ambient air in natural convection:

$$\Phi_{conv} = h_{cv} \times S \times (T_{cu} - T_{amb}) \qquad (9)$$

$$Nu = (h\_cv \times L)/\lambda = k \times ⟦(Gr \times Pr)⟧ \text{ } ^n \qquad (10)$$

In free convection k = 0.52 and n = 0.25. The Grashof and Prandtl numbers are calculated from the thermophysical properties of the air taken at the film temperature.

For the radiative exchanges we calculate the net flux exchanged between the copper and the environment from the relation:

$$\Phi\_rad = \varepsilon \times \sigma \times S \times (T\_cu^4 - T\_amb^4) \qquad (11)$$

The 10/12 copper tube was previously painted in matt black so its emissivity is $\varepsilon = 1$.

We deduced its exchange coefficient h_{rad}. So overall the heat flux exchanged by the copper is:

5

$$\Phi_{emitted} = (h_{cv} + h_{rad}) \times S \times (T_{cu} - T_{amb}) \quad (12)$$

Insteady state and with losses disregarded, this flow must be equal to the electric power consumed. We note a maximum difference of 4% between the measured value of the power of the cartridge and the flow exchanged with the ambient air.

$$\Phi_{emitted} = (h_{cv} + h_{rad}) \times S \times (T_{cu} - T_{amb}) = P \quad (13)$$

Taking again the proposed law for power as a function of voltage ($P = 0.0011 \times U^{1.9895}$) and a similar law for the evolution of $hg = h_{cv} + h_{rad}$ ($h_g = 4.3 \times U^{0.35}$) we can define a relationship linking the temperature to the voltage, that is :

$$T_{cu} = T_{amb} + 0.02 \times U^{1.65} \quad (14)$$

The results obtained are shown in Fig 4. We note a maximum standard deviation of 2.5 for voltage values of 80 and 100 V.

2.5 Test on the Pvc Test Tube

To test our experimental device we applied the procedure to a PVC test tube of the same size as our samples and whose thermal conductivity is given at 0.17 $Wm^{-1}.K^{-1}$.

We drilled radial wells to insert the thermocouples and measured the temperature on the diameters:

d_{cu} = 0.012 m, d_1 = 0.082 m, d_2 = 0.154 m and d_{ex} = 0.164 m.
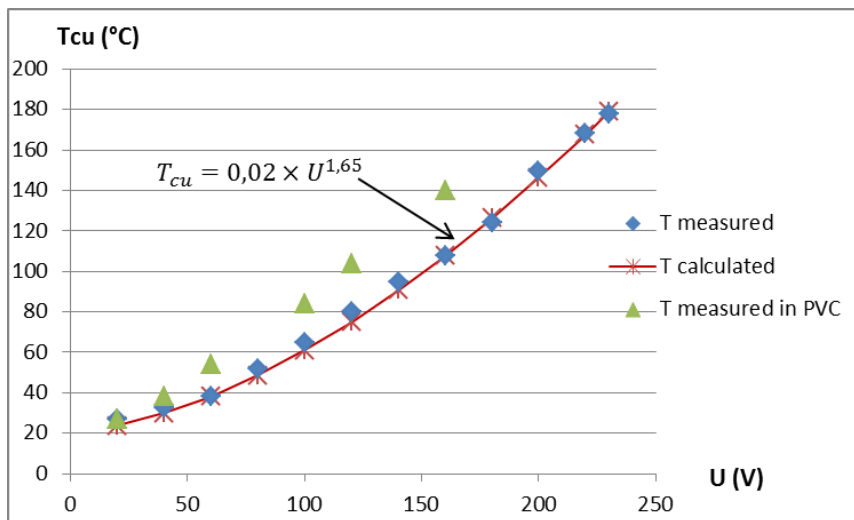

Fig. 4. Temperature versus power

Table 1. Relationship between voltage and thermal flows

	Supplied power - Measured -			Dissipated thermal power - Calculated -				
U (V)	I (mA)	P (W)	T Cu (°C)	Φconv (W)	Φrad (W)	Φemitted (W)	hg (W.m^{-1}.K^{-1})	Uncertainty (%)
20	34.4	0.688	25.8	0.350	0.340	0.690	11.93	-0.291
40	51.5	2.06	33.5	1.150	0.926	2.076	13.76	-0.761
60	67.8	4.068	43.2	2.347	1.727	4.074	15.21	-0.145
80	89.4	7.152	56.5	4.195	2.952	7.147	16.69	0.066
100	106.6	10.66	69.7	6.192	4.324	10.516	17.90	1.348
120	119.2	14.304	82.7	8.277	5.839	14?116	18.96	1.314
140	136.9	19.166	98.4	10.916	7.904	18?820	20?16	1.805
160	156.7	25.072	117	14.178	10.714	24.892	21.49	0.717
180	177	31.86	135.6	17.559	13.956	31.515	22.80	1.084
200	201.8	40.36	158	21.756	18.493	40.249	24.35	0.275
220	218.1	47.982	174.2	24.862	22.247	47.109	25.49	1.820
230	221.2	50.876	181	26.181	23.939	50.130	25.97	1.467

Fig. 5 shows the evolution of the temperature profile in the PVC block as a function of time. From t = 1000 min, we consider that the system is at equilibrium and therefore in steady state.

The calculation of conductivity results from relation (8). Good consistency of results (Table 2) can be noted with a dispersion of less than 5%.

The result of these measurements allows us to consider that our experimental protocol is valid. Special attention must be paid, however, to the position of the thermocouples and their calibration.

For verification, we have calculated the temperature of copper when included in PVC. In steady state, there is conservation ot the heat flow. So we can write the equation:

$$\Phi_{cart} = \left[\frac{T_{cop} - T_{amb}}{R_{ext}}\right]_{air} = \left[\frac{T'_{cop} - T_{amb}}{R_{PVC} + R'_{ext}}\right]_{PVC+air} \quad (15)$$

For U = 80 V, the temperature thus calculated gives T'_{cop} = 71.8°C whereas we have a measurement of 73°C. This difference of 1.6 % comes from the calculation of convective exchange.

A difference of 1°C results in a difference of 5.5% in the value of thermal conductivity while a shift of 1 mm on the diameter will have a repercussion only 10 times lower.

Table 2. shows the calculated conductivity values are independent of the position of the temperature sensors. The low dispersion of the results (1.1%) shows that contact resistances are negligible.

We modeled, in 3D by finite volumes, the dynamic thermal behavior of the PVC block. In the axial direction, the cylinder is split into 5 mm thick discs. In the radial direction, each disk is broken down into 5 mm rings with a time step of 1 s to check the stability criterion:

$\Delta t_i \leq \frac{c_i}{\sum_j \frac{1}{R_{ij}}}$ (which expresses the ratio of the heat

capacity of a node to the inverse of the conductive resistance between nodes).

Fig. 6 shows a good correspondence between calculation and measurement. Analysis of the results from the calculation shows a maximum deviation of 2 degrees between the middle part and the ends of the block (i.e. 1.5%). So the edge effects on the ends of the cylinder are negligible.

2.6 Measurements on Clay Test Specimens

We performed measurements on different formulations as presented in Table 3. With: A for clay, P for straw, S for sand and GA for gum arabic expressed in mass percentages. For each formulation only one sample was made because a quantity of near 10 kg of Tchad's clay is needed and we don't have large quantities in France.

After preparing and drying, the cylinders undergoes three temperature rises, each of them participating to the mean value of thermal conductivity values given here.
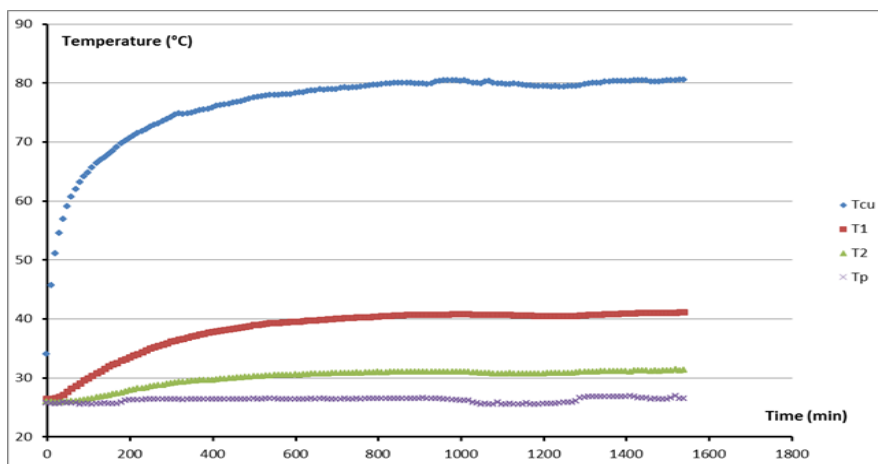

Fig. 5. Temperature versus time for a voltage of 88 V

Table 2. Calculated value of the thermal conductivity of PVC

Measured value							Calculation of λ (mW.m^{-1}.K^{-1}) = f(diameter ratio)						
TCu (°C)	T1 (°C)	T2 (°C)	Tp (°C)	Tamb (°c)	I (mA)	U (V)	d1/dCu	d2/dCu	dp/dCu	d2/d1	dp/d1	dp/d2	λmean
38.0	29.3	26.5	26.2	24.0	40	40	177	176	176	175	175	175	175
48.2	32.0	26.9	26.2	22.2	49.8	57.2	169	170	170	172	172	178	172
53.4	33.7	27.1	26.4	21.0	59.6	62.3	178	179	179	173	172	166	175
81.0	41.0	28.0	25.7	26.3	81	88.6	173	172	172	170	170	173	171
115.5	56.7	35.0	33.0	22.5	100	115	188	181	181	163	164	180	176
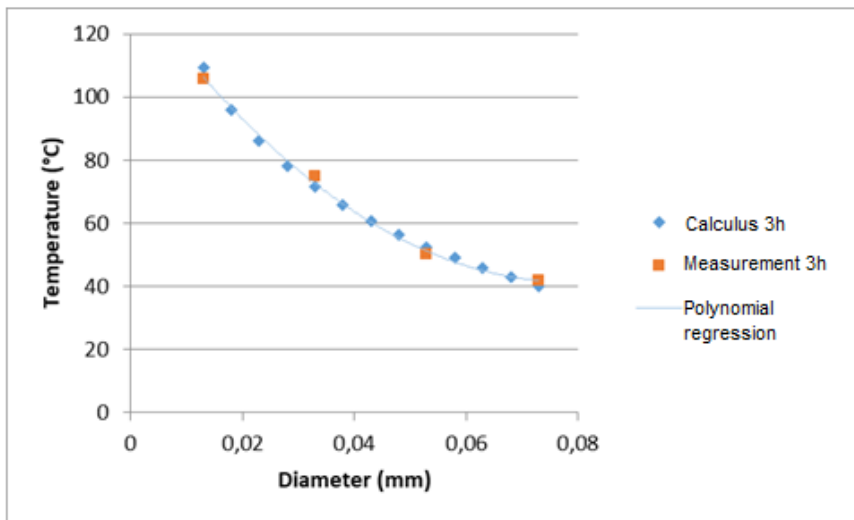
Fig. 6. Comparison: measured values / calculated values

Fig. 7. photography of samples :70%A-30%S, 65%A-30%S-5%GA, A100%, 98.5%A-1.5%P.

3. RESULTS AND DISCUSSION

For each of these formulations we calculated the thermal conductivity for a given installed power when steady state is established. The measurement was repeated 3 to 5 times.

This calculation is made on the basis of temperature readings made every 10 minutes over a period of about 6 hours. The average value over this period will be retained as the final value. These results are shown in Fig. 5.

Table 3. Different formulations tested.

Formulations	Density (kg.m^{-3})	Humidity (%)	Thermal conductivity (W.M^{-1}.K^{-1})
100%A	1888	16.2	0.92
99,5%A – 0,5%P	1757	16.2	0.76
99%A – 1%P	1644	14.9	0.70
98,5%A – 1.5%P	1606	13.6	0.67
70%A – 30%S	1977	14.9	1.40
65%A – 30%S – 5%GA	2033	13.6	0.76
60%A – 30%S – 10%GA	1980	12.4	0.78
55%A – 30%S – 15%GA	1925	11.1	0.93

The humidity measurement is made according to standard NF P94-050 [18]. The moisture content according the dry mass is given by:

$$W\% = \frac{(M_1 - M_2)}{M_2} \times 100 \qquad (16)$$

Where M_1 is the mass before steaming and M_2 the mass after steaming at 105°C for 24 hours.
Clay alone would have a measured thermal conductivity of 0.92 W.m^{-1}.K^{-1}. In the literature [19] it is usually given at 1.1 Wm^{-1}.K^{-1}.

The addition of straw results in a decrease in thermal conductivity. These results are consistent with what is found in the literature [20,21,22]

Fig. 8 shows the evolution of the thermal conductivity of the specimen in relation to the percentage of the stabilizer content. It can be noticed (as with the use of cement [23,24] that it

drops to a content of 5% GA. This decline could be related to the distribution of gum arabic which would be insufficient to promote the establishment of a homogeneous structure.

Beyond 5% GA it rises without reaching the value obtained with clay alone. This variation could be attributed to a strengthening of bonds between sand and clay with the creation of a continuous and more homogeneous internal structure. It would be interesting to measure the porosity of the different formulations to see if there is a cause-and-effect relationship.

The addition of straw to the clay has the effect of reducing the thermal conductivity of our formulations and contributes to slightly lowering the density of the test pieces.

We can see that our results (in red on Fig. 9) correspond quite well to the results presented by the CSTB [25].
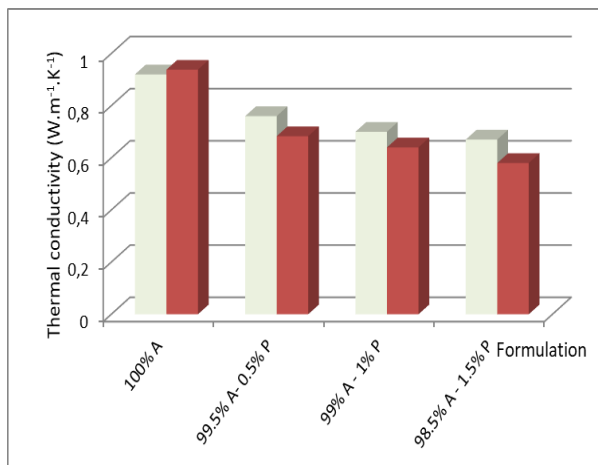
A – With straw
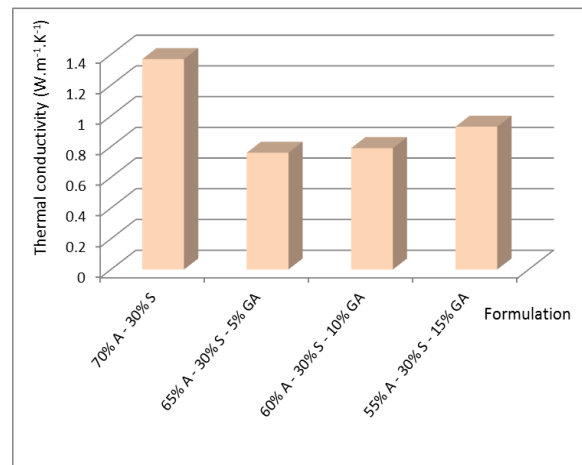
B – With arabic gum

Fig. 8. Measured thermal conductivity values for the different formulations
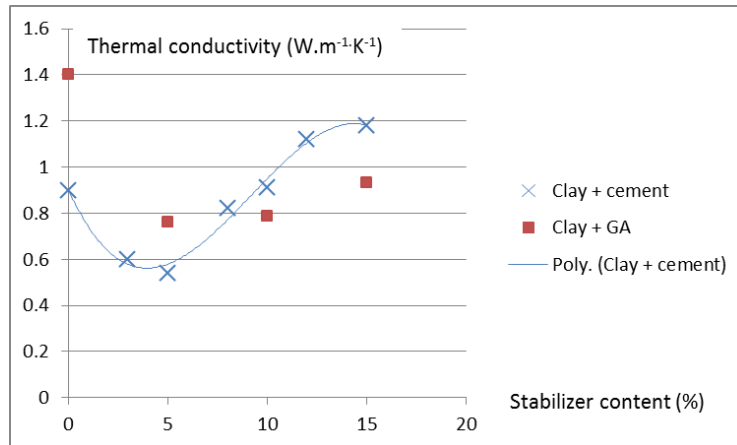
9

Fig. 9. Thermal conductivity versus stabilizer content percentage

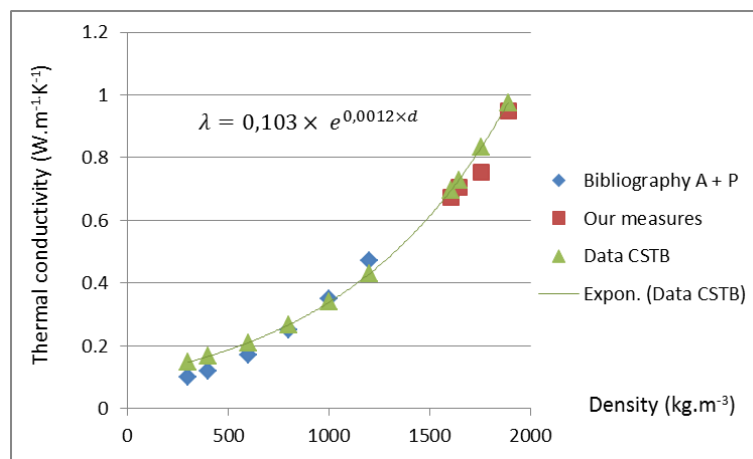$$\lambda = 0{,}103 \times e^{0{,}0012 \times d}$$

Fig. 10. Thermal conductivity versus density

It should be noted, however, that our measurements only concern a small part of the density range because the amount of straw becomes such that the specimens lose their mechanical strength.

4. IMPACT ON THERMAL BEHAVIOR

Overall, our formulations have a thermal conductivity which is between 0.9 W.m^{-1}.K^{-1} and 1.4 W.m^{-1}.K^{-1}. The material can hardly be described as insulating from the thermal point of view.

Our attention is now drawn to the notion of thermal inertia associated with earth walls and we need to verify if the phase shift generated by the material is promising from the point of view of thermal comfort. Indeed, we are dealing with a heavy material; its density is close to 1900 kg.m^{-3} and its thermal capacity is 900 J.kg^{-1}.K^{-1}.

The thermal inertia of a material is evaluated using the following two parameters :

• Thermal diffusivity determines the speed with which the temperature of a material evolves in relation to the external thermal demands;

$$\alpha = \frac{\lambda}{\rho \times c_p} \, [m^2.s^{-1}] \tag{17}$$

• Effusivity is the ability to exchange thermal energy with its environment;

$$E = \sqrt{\lambda \times \rho \times c_p} \, \left[J.K^{-1}.m^{-2}.s^{-1/2} \right] \tag{18}$$

The phase shift is given by the ratio between the thickness of a given wall and celerity.

Celerity, C, represents the rate of diffusion of heat through the wall. It depends on the period of

oscillations of the outside temperature over 24 hours, thus:

$$C = \frac{2 \times \pi}{T \times \sqrt{\frac{\pi}{T}}} \times \sqrt{\alpha} \qquad (19)$$

Phase shift □ is therefore given by :

$$\psi = \frac{e \times T \times \sqrt{\frac{\pi}{T}}}{2 \times \pi \times \sqrt{\alpha}} = \frac{e}{2} \times \sqrt{\frac{T}{\pi \times \alpha}} \qquad (20)$$

Thus for a period T = 24 hours: □ in m².h^{-1}

$$\psi = \frac{e \times 0.023}{\sqrt{\alpha}} \qquad (21)$$

Numerical application: with the α data mentioned at the beginning of the paragraph a phase shift of 6 hours is obtained with a 20 cm thick wall. Below we review in detail the calculations for our different formulations in order to compare them with traditional materials.

Our material (Table 4) has properties quite similar to those of terracotta [26,27,28] with a phase shift of more than 6 hours for a thickness of 20 cm. This phase difference would be sufficient in our latitudes but the material is intended to be used in the region of N'Djamena where a phase shift in the order of 10 hours would be required corresponding to a material thickness of 30 cm.

To confirm these results obtained in the first analysis, we entered our data in a calculation code [29] developed to predict the temperature in a room subjected to solar lighting with a variation in outside temperature. The code is based on the quadrupole method by really taking into account the dynamic regime.

The results of this calculation (Fig. 10) show that with cement, the amplitude of variation of the interior air temperature is 17°C while it is only 6°C with clay. The induced phase shift is 6 to 7 hours in the case of cement whereas it reaches 11 to 12 hours with clay.

A clay wall therefore has the double advantage of reducing the variation in daily temperature and shifting the maximum temperature during the night period. A simple air renewal allows to refresh the internal atmosphere.

Clay, used as a building material, therefore makes it possible to act appreciably on summer comfort and energy management in buildings.
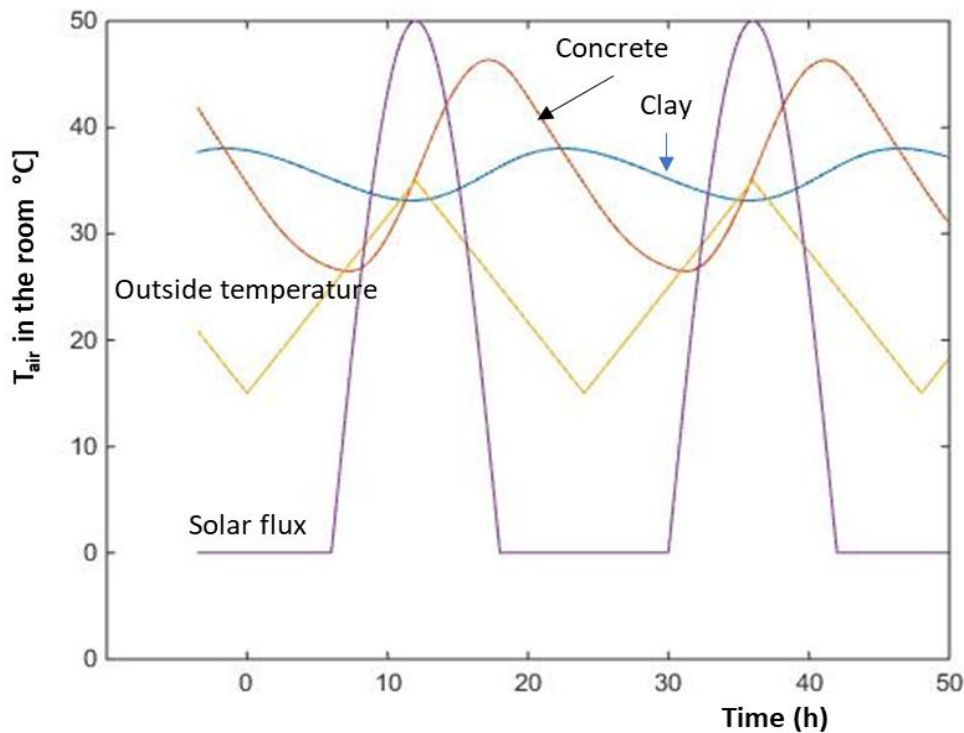

Fig. 11. Evolution of the interior temperature. Concrete - Clay comparison

Table 4. Comparative phase shifts of different materials

Material	Thermal conductivity W.m^{-1}.K^{-1}	Density kg.m^{-3}	Thermal capacity J.kg^{-1}·K^{-1}	Thermal resistance m^2.K.W^{-1}	Thermal diffisivity m^2.s^{-1}	Phase shift h
Concrete block	1.05	1300	650	0.19	1.24E-06	4.13
Terracotta brick	1	1850	1000	0.20	5.40E-07	6.26
Clay brick	1	2000	900	0.20	5.56E-07	6.17
Polystyrene	0.032	15	1450	6.25	1.47E-06	3.79
Our material (CCB) 55%A – 30%S – 15%GA	0.93	1925	925	0.22	5.22E-07	6.37

5. CONCLUSION

The compressive strength results obtained with clay stabilized with 10 to 15% of gum arabic make it possible to conclude positively as to its use in building [2].

The material we propose has an average thermal conductivity of 0.965 with a standard deviation of 0.23. The difference between these kinds of materials and cement or commune thermal insulator like polystyrene is there thermal diffusivity which is near a third from those of cement or polystyrene. Consequently they induce a greater thermal delay than cement or common insulator without noticeably affecting a wall thickness. For example with a wall thickness of 30 cm the inner maximum temperature reach near midnight, when exterior temperature is sufficiently low to refresh naturally the house in regard to cement for which the inner maximum temperature reach near 19h when outer temperature is not sufficient to cool.

For the daily temperature range the clay composite reduces the inner temperature range variation of 3 in regards to cement wich participate to a thermal comfort sensation more regular.

In addition, the availability of raw materials (clay, gum arabic and straw) is abundant and local. The replacement of cement with gum arabic reduces the gray energy contained by the material. As a result, it will help limit damage to the environment.

DISCLAIMER

The products used for this research are commonly and predominantly use products in our area of research and country. There is absolutely no conflict of interest between the authors and producers of the products because we do not intend to use these products as an avenue for any litigation but for the advancement of knowledge. Also, the research was not funded by the producing company rather it was funded by personal efforts of the authors.

COMPETING INTERESTS

Authors have declared that no competing interests exist.

REFERENCES

1. World Bank Data. Open Data, Tchad; 2019.
   Available:https://www.donnees.banquemondiale.org/Contry/Tchad/2019
2. Abakar A, Benelmir R, Tanguier JL, et al. Abdoulaye Saleh. Caractéristiques mécaniques de l'argile de N'Djamena stabilisée par la gomme arabique. Afrique science. 2017;12.
3. Abakar Ali, Jean-louis Tanguier, Riad Benelmir et Abdoulaye Todjibal. Caractéristiques mécaniques de bloc de terre comprimée (BTC) stabilisée par la gomme arabique. Afrique science. 2019; 15(1).
4. Filati M. Conductivité apparente des milieux granulaires soumis à des contraintes mécaniques: Modélisation et mesures. Thèse INPT; 2006.
5. Damfeu JC, Meukam P, Jannot Y. Modeling and measuring of the thermal properties of insulating vegetable fibers by the asymmetrical hot plate method and the radial flux method: Kapok, coconut, groundnut shell fiber and rattan. Thermochimica Acta. 2016;630:64-77.
6. Inseok Yang, Daeho Kil, Sanghyun Lee. Construction and preliminary testing of a guarded hot plate apparatus for thermal

conductivity measurements at high temperatures. International Journal of Heat and Mass Transfer. 2018;122:1343-1352.

7. Norme ISO 8302. Isolation thermique - Détermination de la résistance thermique et des propriétés connexes en régime stationnaire - Méthode de la plaque chaude gardée; 1991.

8. Dongliang Zhao, Xin Qian, Xiaokun Gu, SaadAyubJajja, Ronggui Yang. Measurement Techniques for Thermal Conductivity and Interfacial Thermal Conductanceof Bulk and Thin Film Materials. Department of Mechanical Engineering, University of Colorado, Boulder, CO 80309-0427; 2020.

9. Reddy KS. Jayachandran S. Investigations on design and construction of a square guarded hot plate (SGHP) apparatus for thermal conductivity measurement of insulation materials. International Journal of Thermal Sciences. 2017;120:136-147.

10. Rayed Alyousef, Omrane Benjeddou, ChokriSoussi, Mohamed Amine Khadimallah, Malek Jedidi. Experimental Study of New Insulation Lightweight Concrete Block Floor Based on Perlite Aggregate, Natural Sand, and Sand Obtained from Marble Waste. Advances in Materials Science and Engineering. 2019;14.
Article ID 8160461.

11. Jedidi M, Benjeddou O, Soussi C. Effect of expanded perlite aggregate dosage on properties of lightweight concrete. Jordan Journal of Civil Engineering. 2015;9(3): 278-291.

12. Yoon S, Macphee DE, Imbabi MS. Estimation of the thermal properties of hardened cement paste on the basis of guarded heat flow meter measurements. Thermochimica Acta. 2014;588:1-10.

13. Muhammad B. Ahmed, Salwa Shaik, Ankur Jain. Measurement of radial thermal conductivity of a cylinder using a time-varying heat flux method. International Journal of Thermal Sciences. 2018;129: 301-308.

14. Jannot Y, Degiovanni A, Payet G. Thermal conductivity measurement of insulating materials with a three layers device, International Journal of Heat and Mass Transfer. 2009;52:1105-1111.

15. Carlson JD, Bhardwaj R, Phelan PE, Kaloush KE, Golden JS. Determining thermal conductivity of paving materials using cylindrical sample geometry. Journal of materials in civil ingineering. 2010; 22(2):186-195.

16. Norme Européenne NF EN 12390-1. Essais pour bétons durcis. Forme, dimensions et autres exigences relatives aux éprouvettes et aux moule; 2012.

17. Philippe Cosenza, Roger Ghérin, Alain Tabbagh. Relationship between thermal conductivity and water content of soils using numerical modeling. European Journal of Soil Science. 2003;54(3):581-588.

18. Norme NF P94-050, Sols: Reconnaissance et essais. Détermination de la teneur en eau pondérale des matériaux. Méthode par étuvage; 1995.

19. Nan Zhang, Zhaoyu Wang. Review of soil thermal conductivity and predictive models. International journal of thermal science. 2017;117:172-183.

20. Yassine Elhamdouni, Abdelhamid Khabbazi, Chaimaa Benayad, Abdallah Dadi, Oumar Idriss Ahmid. Effect of fiber alfa on thermophysical characteristics of a material based on clay. Energy Procedia. 2015;74:718-727.

21. El Azhary K, Chihab Y, Mansour M, Laaroussi N, Garoum M. Energy efficiency and thermal properties of the composite material clay-straw. Energy procedia. 2017;141:160-164.

22. Mohammed Lamrani, Majid Mansour, Najma Laaroussi, Mohamed Khalfaoui. Thermal study of clay bricks reinforced by three ecological materials in south of morocco. Energy procedia. 2019;156:273-277.

23. Tha Ashour, Azra Korjenic, Sinan Korjenic, Wei Wu. Thermal conductivity of unfired bricks reinforced by agricultural wastes with cement and gypsum. Energy and buildings. 2015;104: 139-146.

24. Moro Olivier Boffoue, Koffi Clément Kouadio, Conand Hinoré Kouakou, Aka Alexandre Assande, Anne Dauscher, Bertrand Lenoir, Edjikemé Emeruwa. Influence de la teneur en ciment sur les propriétés thermomécaniques des blocs d'argile comprimée et stabilisée. Afrique science. 2015;11(2):35-43.

25. Quenard D, Propriétés hygrothermiques de la terre crue, CSTB/Enveloppe et revêtements / Physique des matériaux. Journée terre crue; 2008.

26. Mohamed Ben Mansour, Ahmed Jelidi, AmelSoukaina, Sadock Ben Jabrallah.

Optimizing thermal and mechanical performance of compressed earth blocs (CEB). Construction and building materials. 2016;104:44-51.

27. Rémi Bouchié, Benoit Busson, Franck Leguillon, Kamel Zibouche. RT : Valeurs et coefficients pour l'application des règles Th-Bat. Centre Scientifique et Technique du Bâtiment (CSTB). 2018;504. ISBN13 : 978-2-86891-690-7.

28. Bwayo E, Obwoya SK. Coefficient of thermal diffusivity of insulation brick developed from sawdust and clays. Journal of Ceramics; 2014. ID 861726.

29. Maillet D, André S, Batsale JC, Degiovanni A, Moyne C. Thermal Quadrupoles: Solving the Heat Equation through Integral Transforms. New York: John Wiley and Sons; 2012.

Greatings: